



Combined DØ Upper Limits on Standard-Model Higgs-Boson Production

The DØ Collaboration
URL <http://www-d0.fnal.gov>
(Dated: August 2, 2006)

Upper limits on the cross section for Standard-Model Higgs-boson production in $p\bar{p} \rightarrow H + X$ at $\sqrt{s} = 1.96$ TeV are determined for $100 < m_H < 200$ GeV/ c^2 . The contributing processes include associated production ($WH \rightarrow \ell\nu b\bar{b}$, $ZH \rightarrow \ell^+\ell^-/\nu\bar{\nu}b\bar{b}$, and $WH \rightarrow WW^+W^-$) and gluon fusion ($H \rightarrow W^+W^-$). Analyses are conducted with integrated luminosities from 260 pb $^{-1}$ to 950 pb $^{-1}$ recorded by the DØ experiment. Limits for various combinations of the channels are presented. The results are in good agreement with background expectations and the 95% CL upper limits are found to be a factor of 16.3(4.3) higher than the Standard-Model cross section at $m_H = 115(160)$ GeV/ c^2 .

Preliminary Results for Summer 2006 Conferences

TABLE I: List of analysis channels, corresponding integrated luminosities, and final variables.

| Channel | Luminosity (pb ⁻¹) | Final Variable | Reference |
|--|--------------------------------|---------------------------------|-----------|
| $WH \rightarrow e\nu b\bar{b}$, ST/DT | 371 | Dijet mass | [16] |
| $WH \rightarrow \mu\nu b\bar{b}$, ST/DT | 385 | Dijet mass | [16] |
| $WH \rightarrow \ell\nu b\bar{b}$, ST/DT | 260 | Dijet mass | [17] |
| $WH \rightarrow WW^+W^-(e^\pm e^\pm)$ | 384 | Likelihood discriminant | [19] |
| $WH \rightarrow WW^+W^-(e^\pm \mu^\pm)$ | 368 | Likelihood discriminant | [19] |
| $WH \rightarrow WW^+W^-(\mu^\pm \mu^\pm)$ | 363 | Likelihood discriminant | [19] |
| $ZH \rightarrow \nu\bar{\nu} b\bar{b}$, ST/DT | 260 | Dijet mass | [17] |
| $ZH \rightarrow \mu^+ \mu^- b\bar{b}$, DT | 320 | Dijet mass | [18] |
| $ZH \rightarrow e^+ e^- b\bar{b}$, DT | 389 | Dijet mass | [18] |
| $H \rightarrow W^+W^-(e^+e^-)$ | 950 | $\Delta\varphi(e^+, e^-)$ | [20] |
| $H \rightarrow W^+W^-(e^\pm \mu^m p)$ | 950 | $\Delta\varphi(e^\pm, \mu^\mp)$ | [20] |
| $H \rightarrow W^+W^-(\mu^+ \mu^-)$ | 950 | $\Delta\varphi(\mu^+, \mu^-)$ | [21] |

I. INTRODUCTION

Despite its success as a predictive tool, the Standard-Model (SM) of particle physics remains incomplete without a means to explain electroweak-symmetry breaking. The simplest proposed mechanism involves the introduction of a complex double of scalar fields that generate particle masses via their mutual interactions. After accounting for longitudinal polarizations in the electroweak sector, this so-called Higgs mechanism also gives rise to a single scalar boson with an unpredicted mass. Direct searches in $e^+e^- \rightarrow Z^* \rightarrow ZH$ at the Large Electron Positron (LEP) collider yielded lower mass limits at $m_H > 114.4$ GeV/c²[1]. The SM Higgs boson search remains a large portion of the Fermilab Tevatron physics program.

In this note, we combine results for direct searches for SM Higgs bosons in $p\bar{p}$ collisions at $\sqrt{s} = 1.96$ TeV recently presented by DØ [2]. These are searches for Higgs bosons produced in association with vector bosons ($p\bar{p} \rightarrow W/ZH \rightarrow \ell\nu b\bar{b}/\nu\bar{\nu} b\bar{b}$, $p\bar{p} \rightarrow WH \rightarrow WW^+W^-$) or singly through gluon-gluon fusion ($p\bar{p} \rightarrow H \rightarrow W^+W^-$). The searches were conducted with data collected during the period 2003-2005 and correspond to integrated luminosities ranging from 260 pb⁻¹ to 950 pb⁻¹ and separated into sixteen final states, referred to as analyses in the following. Each analysis is designed to isolate a particular final state defined by a Higgs boson production and decay mode. In order to ensure proper combination of signals, the analyses were designed to be mutually exclusive after analysis selections.

The sixteen analyses[16-21] are categorized by their production processes and outlined in Table I. In the cases of $p\bar{p} \rightarrow W/ZH$ production, we search for both $H \rightarrow b\bar{b}$ and $H \rightarrow W^+W^-$ decays. For the $H \rightarrow b\bar{b}$ decays, the analyses are separated into two orthogonal groups: one in which two of the b -quarks were tagged via b -jet identification or b -tagging (herein called double-tag or DT) and one group in which only one b -quark was tagged (single-tag or ST)[23]. The decays of the vector bosons further define the analyzed final states: $WH \rightarrow e\nu b\bar{b}$, $WH \rightarrow \mu\nu b\bar{b}$, $ZH \rightarrow \ell^+\ell^- b\bar{b}$, and $ZH \rightarrow \nu\bar{\nu} b\bar{b}$. There is a sizable amount of $WH \rightarrow \ell\nu b\bar{b}$ signal that can mimic the $ZH \rightarrow \nu\bar{\nu} b\bar{b}$ final state when the lepton is undetected. This case is treated as a separate WH analysis, to which we refer as $WH \rightarrow \ell\nu b\bar{b}$. We also include an analysis of $WH \rightarrow WW^+W^-$ final states. Here the associated W boson and the same-charged W boson from the Higgs decay semi-leptonically, thus defining six final states: $WH \rightarrow We^\pm\nu e^\pm\nu$, $We^\pm\nu\mu^\pm\nu$, and $W\mu^\pm\nu\mu^\pm\nu$. All decays of the third W boson are included. In the case of $p\bar{p} \rightarrow H \rightarrow W^+W^-$ production, we again search for semi-leptonic W boson decays with four final states: $WW \rightarrow e^+\nu e^-\nu$, $e^\pm\nu\mu^\mp\nu$, and $\mu^+\nu\mu^-\nu$. For the gluon fusion process, $H \rightarrow b\bar{b}$ decays are not considered due to the large multijets background.

All Higgs signals are simulated using PYTHIA v6.202[3] using CETQ5L[4] leading order parton distribution functions. The signal cross sections are normalized to next-to-next-to-leading order calculations[5, 6] and branching ratios are calculated using HDECAY[7]. The expected contributions from multijet backgrounds (QCD production) are measured in data. For the DØ analyses, the other backgrounds were generated by PYTHIA, ALPGEN, and COMPHEP[10], with PYTHIA providing parton-showering and hadronization for all. Background cross sections were normalized to next-to-leading order calculations from MCFM[11] in all possible cases.

II. LIMIT CALCULATIONS

We combine results using the CL_s method with a log-likelihood ratio (LLR) test statistic[12]. This method provides a robust means of combining individual channels while incorporating systematic uncertainties. Systematics are treated

as uncertainties on the expected numbers of signal and background events, not the outcomes of the limit calculations. This approach ensures the the uncertainties and their correlations are propagated to the outcome with their proper weights. The CL_s approach used here utilizes binned final-variable distributions rather than a single-bin (fully-integrated) value.

A. Final Variable Preparation

In the case of the $H \rightarrow b\bar{b}$ analyses, the final variable used for limit setting is the invariant dijet mass, either when only one of the two jets used for the dijet mass is tagged as a b -jet, or when both jets are b -tagged. Examples of these two types of distributions are given in Figs 1a,b. In the $H \rightarrow W^+W^-$ analyses, the Higgs mass cannot be directly reconstructed due to the neutrinos in the final state. Thus, the $WH \rightarrow WW^+W^-$ analysis uses a likelihood discriminant formed from topological variables as a final variable, as shown in Fig. 1b, and the $p\bar{p} \rightarrow H \rightarrow W^+W^-$ analysis uses the difference in φ between the two final state leptons ($\Delta\varphi(\ell_1, \ell_2)$), as shown in Fig. 1c.

Each signal and background final variable is smoothed via Gaussian kernel estimation[13]. In a few instances, the statistics of a Monte Carlo (MC)-derived background source are too small to properly described the expected shape of the final-variable distribution. In these cases, the shape is taken from a higher statistics sample of the same background and the proper normalization is applied. For example, after applying a double b -tag selection in the $WH \rightarrow \mu\nu b\bar{b}$ analysis, the dijet mass final variable for the $W + 2$ jet background retains only four events. The resulting dijet mass spectrum is thus insufficiently populated to reliably estimate the shape for this background. To partially correct for this effect, the background shape is taken from the $W + 2$ jet single-tag selection with the double-tag normalization applied. In this manner, the systematic uncertainty associated with the shape of this final variable is greatly reduced[14].

To decrease the granularity of the steps between simulated Higgs masses in the limit calculation, additional Higgs mass points are created via signal point interpolation[15]. The primary motivation of this procedure is to provide a means of combining analyses which do not share a common simulated Higgs mass. However, this procedure also allows a measurement of the behavior of each limit on a finer granularity than otherwise possible.

B. Systematic Uncertainties

The systematic uncertainties differ between analyses for both the signals and backgrounds[16-21]. Here we will summarize only the largest contributions. All analyses carry an uncertainty on the integrated luminosity of 6.5%. The $H \rightarrow b\bar{b}$ analyses have an uncertainty on the b -tagging rate of 4-6% per tagged jet. These analyses also have an uncertainty on the jet measurement and acceptances of $\sim 7.5\%$. For the $H \rightarrow W^+W^-$ and $WH \rightarrow WW^+W^-$ analyses, the largest uncertainties are associated with lepton measurement and acceptances. These values range from 3-6% depending on the final state. The largest contributing factors for all analyses is the uncertainty on the background cross sections at 6-19% depending on the background[24]. More complete details for systematic uncertainties are given in Table II.

The systematic uncertainties for the background rates are generally several times larger than the signal expectation itself and are thus an important factor in the calculation of limits. As such, each systematic uncertainty is folded into the signal and background expectations via Gaussian distribution. These Gaussian values are sampled for each Poisson MC trial (pseudo-experiment). Correlations between systematic sources are carried through in the calculation. For example, the uncertainty on the integrated luminosity is held to be correlated between all signals and backgrounds and, thus, the same fluctuation in the luminosity is common to all channels for a single MC trial. All systematic uncertainties originating from a common source are held to be correlated, as detailed in Table II.

III. DERIVED UPPER LIMITS

We derive limits on SM Higgs boson production $\sigma \times BR(H \rightarrow X)$ via sixteen individual analyses[16-21]. These analyses are first grouped by final state to produce individual results. We group channels by production modes to form combined results. The limits are derived at a confidence level (CL) of 95%. To facilitate model transparency and to accommodate analyses with different degrees of sensitivity, we present our results in terms of the ratio of limits set to the SM cross sections ($\sigma \times BR(H \rightarrow X)$) as a function of Higgs mass. The SM prediction for Higgs boson production would therefore be considered excluded at 95% CL when this limit ratio falls below unity.

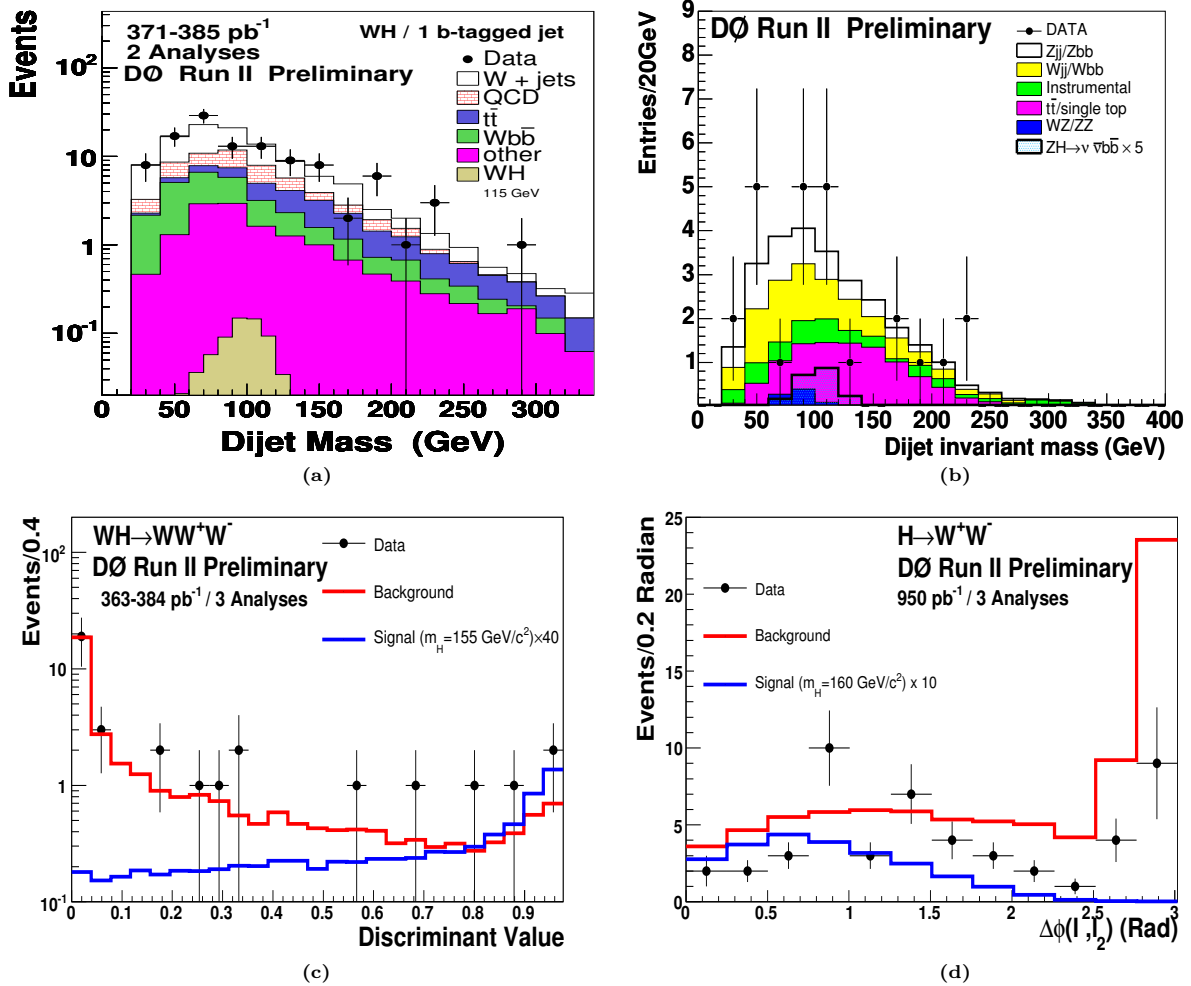


FIG. 1: Final variable distributions for selected Higgs search analyses. Shown in the figure are distributions for: the dijet invariant mass for $WH \rightarrow e, \mu\nu b\bar{b}$ ST analyses (a), the dijet invariant mass for the $ZH \rightarrow \nu\bar{\nu}b\bar{b}$ DT analysis (b), the likelihood discriminant for the $WH \rightarrow WW^+W^-$ analyses (c), and $\Delta\varphi(\ell_1, \ell_2)$ for the $H \rightarrow W^+W^-$ analyses (d). For all figures, background expectations and observed data are shown. The expected Higgs signals at selected masses are scaled as indicated.

A. Results for Individual Channels

Figure 2 shows the LLR distributions for $WH(H \rightarrow b\bar{b}, \text{ST}+\text{DT})$, $ZH \rightarrow \ell^+\ell^-/\nu\bar{\nu}b\bar{b}(\text{ST}+\text{DT})$, $WH \rightarrow WW^+W^-$, and $H \rightarrow W^+W^-$ final states, respectively. Included in these figures are the LLR values for the signal+background hypothesis (LLR_{s+b}), background-only hypothesis (LLR_b), and the observed data (LLR_{obs}). The shaded bands represent the 1 and 2 standard deviation (σ) departures for LLR_b . These distributions can be interpreted as follows:

- The separation between LLR_b and LLR_{s+b} provides a measure of the overall power of the search. This is the ability of the analysis to discriminate between the $s+b$ and b -only hypotheses.
- The width of the LLR_b distribution (shown here as 1 and 2 standard deviation (σ) bands) provides an estimate of how sensitive the analysis is to a signal-like fluctuation in data, taking account of the presence of systematic uncertainties. For example, when a 1- σ background fluctuation is large compared to the signal expectation, the analysis sensitivity is thereby limited.
- The value of LLR_{obs} relative to LLR_{s+b} and LLR_b indicates whether the data distribution appears to be more signal-like or background-like. As noted above, the significance of any departures of LLR_{obs} from LLR_b can be evaluated by the width of the LLR_b distribution.

TABLE II: List of leading correlated systematic uncertainties. The values for the systematic uncertainties are the same for the $ZH \rightarrow \nu\bar{\nu}b\bar{b}$ and $WH \rightarrow \ell\nu b\bar{b}$ channels. All uncertainties within a group are considered 100% correlated across channels. The correlated systematic uncertainty on the background cross section (σ) is itself subdivided according to the different background processes in each analysis.

| Source | $WH \rightarrow e\nu b\bar{b}$ DT(ST) | $WH \rightarrow \mu\nu b\bar{b}$ DT(ST) | $H \rightarrow W^+W^-, WH \rightarrow WW^+W^-$ |
|-------------------------|---------------------------------------|---|--|
| Luminosity (%) | 6.5 | 6.5 | 6.5 |
| Jet Energy Scale (%) | 4.0 | 5.0 | 3.0 |
| Jet ID (%) | 6.8 | 6.8 | 0 |
| Electron ID (%) | 6.6 | 0 | 2.3 |
| Muon ID (%) | 0 | 4.9 | 7.7 |
| b -Jet Tagging (%) | 8.5(5.0) | 8.5(5.0) | 0 |
| Background σ (%) | 6-19 | 6-19 | 6-19 |

| Source | $ZH \rightarrow \nu\bar{\nu}b\bar{b}$ DT(ST) | $ZH \rightarrow e^+e^-b\bar{b}$ | $ZH \rightarrow \mu^+\mu^-b\bar{b}$ |
|-------------------------|--|---------------------------------|-------------------------------------|
| Luminosity (%) | 6.5 | 6.5 | 6.5 |
| Jet Energy Scale (%) | 6.0 | 7.0 | 2.0 |
| Jet ID (%) | 7.1 | 7.0 | 5.0 |
| Electron ID (%) | 0 | 8.0 | 0 |
| Muon ID (%) | 0 | 0 | 12.0 |
| b -Jet Tagging (%) | 9.6(6.7) | 12.0 | 22.0 |
| Background σ (%) | 6-19 | 6-19 | 6-19 |

B. Combined Results

The individual analyses described above can be grouped to form several combined limits:

- All WH searches (ST, DT, and $WH \rightarrow WW^+W^-$) in the low mass range ($m_H = 100 - 145 \text{ GeV}/c^2$).
- All ZH searches (ST and DT) in the low mass range ($m_H = 100 - 145 \text{ GeV}/c^2$).
- All WH , ZH and $H \rightarrow W^+W^-$ searches over the full mass range ($m_H = 100 - 200 \text{ GeV}/c^2$).

Figures 3 and 4 show the expected and observed 95% CL cross section ratios for the combined WH analyses ($WH \rightarrow e, \mu, \ell\nu b\bar{b}$ (ST+DT), and $WH \rightarrow WW^+W^-$) and the combined ZH analyses ($ZH \rightarrow e^+e^-, \mu^+\mu^-, \nu\bar{\nu}b\bar{b}$, ST+DT), respectively, in the mass range $m_H = 100 - 145 \text{ GeV}/c^2$. Figures 5 and 6 show the expected and observed 95% CL cross section ratios for all analyses combined in the low- and high-mass regions, respectively ($m_H = 100 - 145 \text{ GeV}/c^2$ and $m_H = 100 - 200 \text{ GeV}/c^2$). The LLR distribution for the full combination is shown in Fig. 7.

Compared to earlier studies on simulation that also covered the full mass range [22], our results, which use more channels and study them on a wider mass range, show that the region between $m_H = 115 - 190 \text{ GeV}/c^2$ is proved more uniformly than predicted. Indeed there is only a factor of 2 difference in sensitivity between the most and the least sensitive region in this mass range.

IV. CONCLUSIONS

We have presented results for sixteen Higgs search analyses. We have combined these analyses to form new limits more sensitive than each individual limit.

- Combined observed (expected) 95% CL limit ratios to SM cross sections on $p\bar{p} \rightarrow WH, H \rightarrow b\bar{b}/W^+W^-$ range from 20.7(24.3) at $m_H = 115 \text{ GeV}/c^2$ to 62.8(58.2) at $m_H = 135 \text{ GeV}/c^2$.
- Combined observed (expected) 95% CL limit ratios to SM cross sections on $p\bar{p} \rightarrow ZH, H \rightarrow b\bar{b}$ range from 37.4(31.3) at $m_H = 115 \text{ GeV}/c^2$ to 86.9(68.8) at $m_H = 135 \text{ GeV}/c^2$.
- Fully combined observed (expected) 95% CL limit ratios to SM cross sections on $p\bar{p} \rightarrow WH/ZH/H, H \rightarrow b\bar{b}/W^+W^-$ range from 16.3(16.7) at $m_H = 115 \text{ GeV}/c^2$, 4.3(5.9) at $m_H = 160 \text{ GeV}/c^2$, and 13.0(19.5) at $m_H = 200 \text{ GeV}/c^2$.

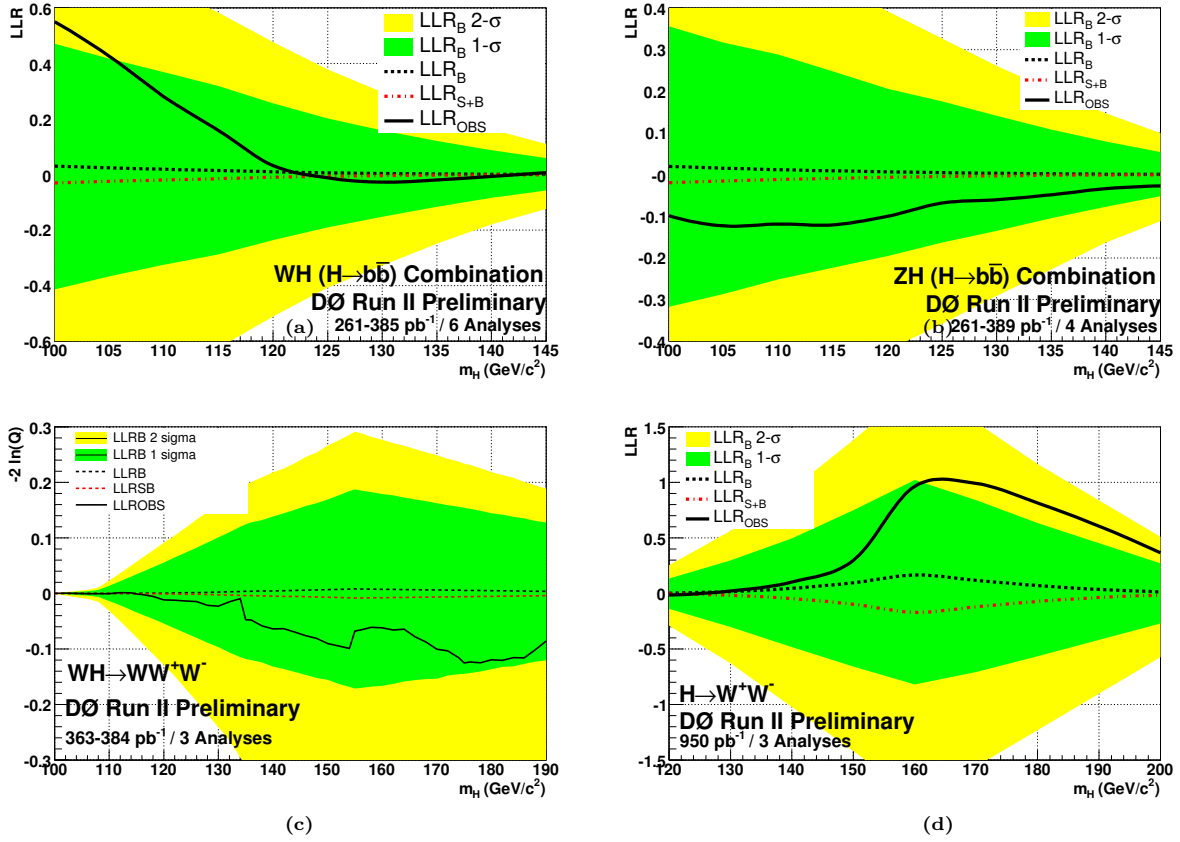


FIG. 2: Log-likelihood ratio distribution for the $WH(H \rightarrow b\bar{b})$ analyses ($WH \rightarrow e, \mu, \ell\nu b\bar{b}$, ST+DT final states combined) (a), the $ZH \rightarrow \ell^+\ell^-/\nu\bar{\nu}b\bar{b}$ ST+DT combined channels (b), the $WH \rightarrow WW^+W^-$ analyses ($e^\pm e^\pm$, $e^\pm \mu^\pm$, and $\mu^\pm \mu^\pm$ final states combined) (c), and the $H \rightarrow W^+W^-$ analyses (e^+e^- , $e^\pm \mu^\mp$, and $\mu^+\mu^-$ final states combined) (d).

These relatively high cross section ratios will decrease strongly in the near future with the luminosity recorded at the Tevatron: more than 1fb^{-1} is currently being analyzed and 8fb^{-1} is expected by the end of 2009. Furthermore, we are developing new techniques to improve the current sensitivity: we expect improvements via multivariate analyses ($\sim 30\%$ increase in sensitivity), neural-network b -tagging ($\sim 35\%$), and improved dijet mass resolution ($\sim 35\%$ for $m_H < 150 \text{ GeV}/c^2$). In addition, an anticipated combination with the results from the CDF collaboration would yield an increase in sensitivity of $\sim 40\%$. As such, we are optimistic about the near-future prospects of the SM Higgs search at the Tevatron.

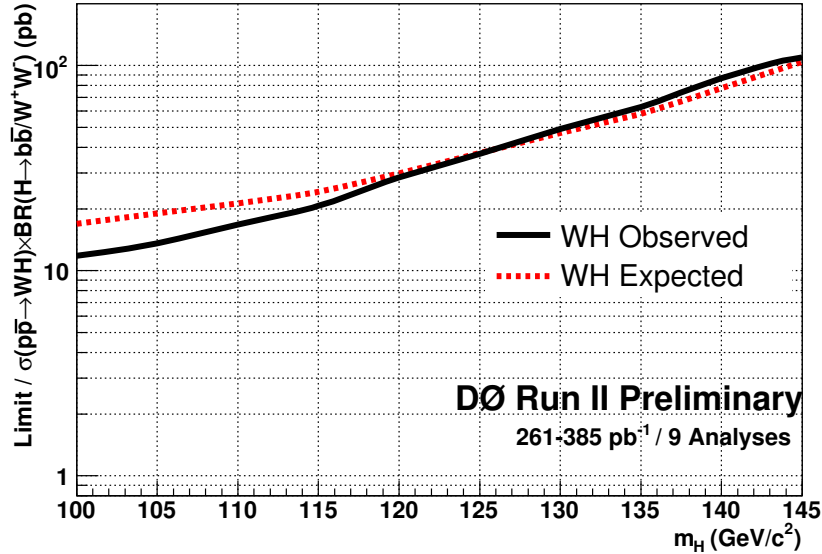


FIG. 3: Expected (median) and observed 95% CL cross section ratios for the combined WH analyses (ST, DT, and $WH \rightarrow WW^+W^-$) in the $m_H = 100 - 145 \text{ GeV}/c^2$ mass range.

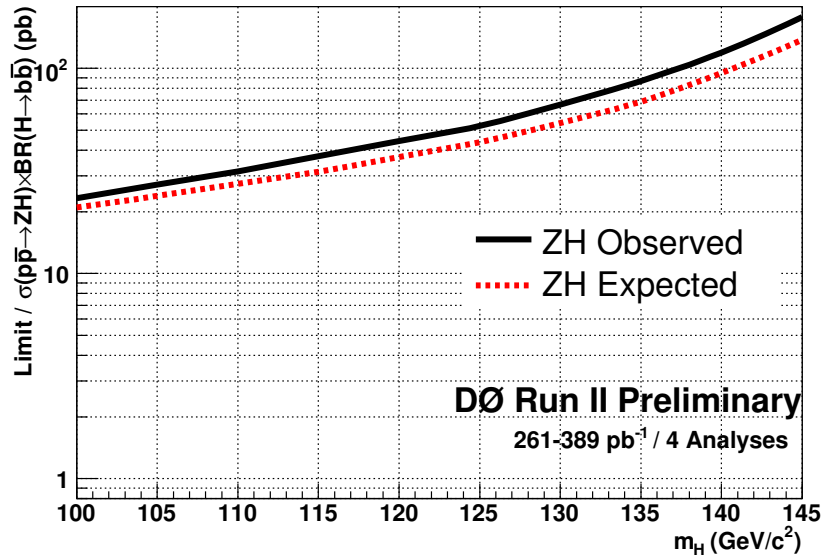


FIG. 4: Expected (median) and observed 95% CL cross section ratios for the combined ZH analyses (ST+DT) in the $m_H = 100 - 145 \text{ GeV}/c^2$ mass range.

Acknowledgments

We thank the staffs at Fermilab and collaborating institutions, and acknowledge support from the DOE and NSF (USA); CEA and CNRS/IN2P3 (France); FASI, Rosatom and RFBR (Russia); CAPES, CNPq, FAPERJ, FAPESP and FUNDUNESP (Brazil); DAE and DST (India); Colciencias (Colombia); CONACyT (Mexico); KRF and KOSEF (Korea); CONICET and UBACyT (Argentina); FOM (The Netherlands); PPARC (United Kingdom); MSMT (Czech Republic); CRC Program, CFI, NSERC and WestGrid Project (Canada); BMBF and DFG (Germany); SFI (Ireland);

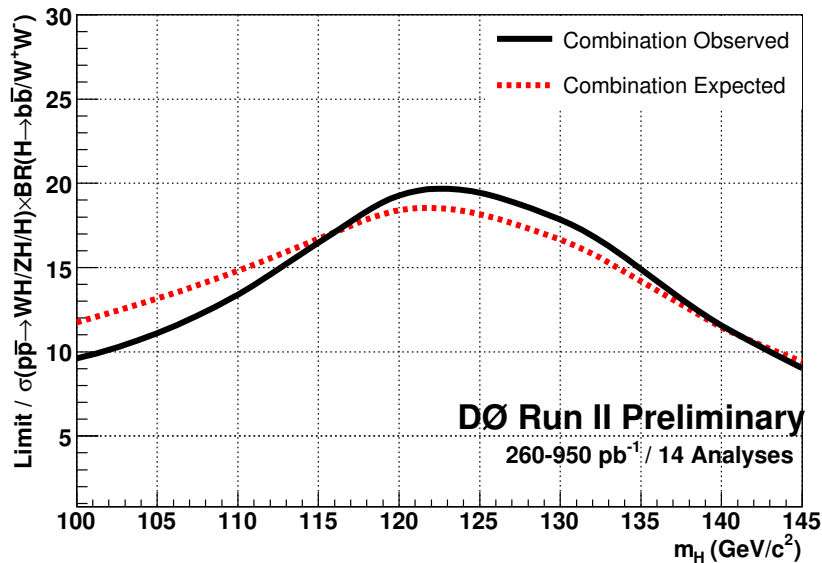


FIG. 5: Expected (median) and observed 95% CL cross section ratios for the combined $WH/ZH/H \rightarrow W^+W^-$ analyses in the $m_H = 100 - 145 \text{ GeV}/c^2$ mass range.

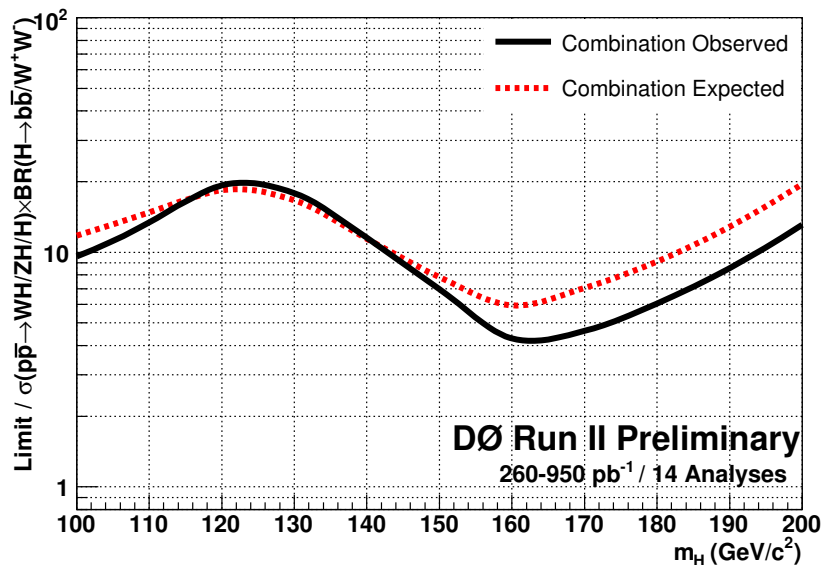


FIG. 6: Expected (median) and observed 95% CL cross section ratios for the combined $WH/ZH/H \rightarrow W^+W^-$ analyses in the $m_H = 100 - 200 \text{ GeV}/c^2$ mass range.

Research Corporation, Alexander von Humboldt Foundation, and the Marie Curie Program.

-
- [1] R. Barate *et al.* [LEP Working Group for Higgs boson searches], Phys. Lett. B **565**, 61 (2003), [arXiv:hep-ex/0306033]
 [2] DØ Collaboration, V. Abazov *et al.*, “The Upgraded DØ Detector”, submitted to Nucl. Instrum. Methods Phys. Res. A, [arXiv:hep-ex/0507191]
 [3] T. Sjostrand, L. Lonnblad and S. Mrenna, “PYTHIA 6.2: Physics and manual,” [arXiv:hep-ph/0108264]

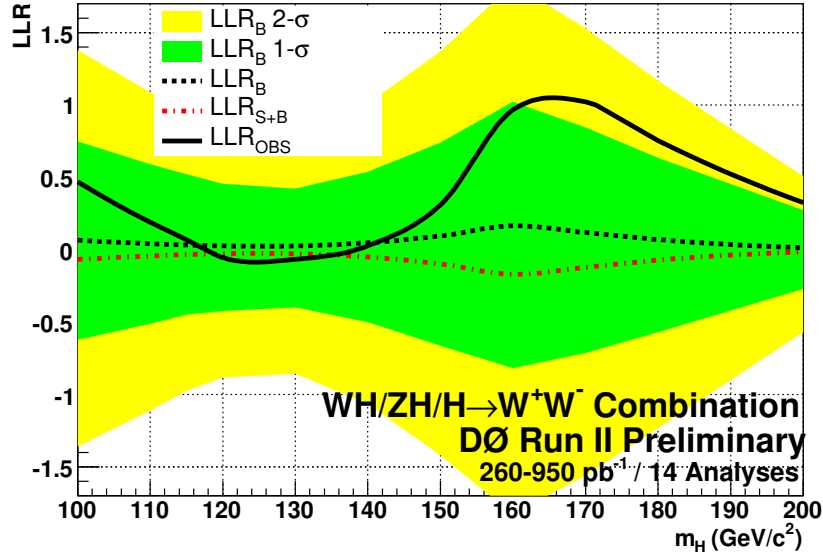


FIG. 7: Log-likelihood ratio distribution for the combined $WH/ZH/H \rightarrow W^+W^-$ analyses in the $m_H = 100-200 \text{ GeV}/c^2$ mass range.

- [4] H. L. Lai *et al.*, “Improved Parton Distributions from Global Analysis of Recent Deep Inelastic Scattering and Inclusive Jet Data”, *Phys. Rev D* **55** 1280 (1997)
- [5] S. Catani, D. de Florian, M. Grazzini and P. Nason, “Soft-gluon resummation for Higgs boson production at hadron colliders,” *JHEP* **0307**, 028 (2003), [arXiv:hep-ph/0306211]
- [6] K. A. Assamagan *et al.* [Higgs Working Group Collaboration], “The Higgs working group: Summary report 2003,” [arXiv:hep-ph/0406152]
- [7] A. Djouadi, J. Kalinowski and M. Spira, “HDECAY: A program for Higgs boson decays in the standard model and its supersymmetric extension,” *Comput. Phys. Commun.* **108**, 56 (1998) [arXiv:hep-ph/9704448]
- [8] M. L. Mangano, M. Moretti, F. Piccinini, R. Pittau and A. D. Polosa, “ALPGEN, a generator for hard multiparton processes in hadronic collisions,” *JHEP* **0307**, 001 (2003) [arXiv:hep-ph/0206293]
- [9] G. Corcella *et al.*, “HERWIG 6: An event generator for hadron emission reactions with interfering gluons (including supersymmetric processes),” *JHEP* **0101**, 010 (2001) [arXiv:hep-ph/0011363]
- [10] A. Pukhov *et al.*, “CompHEP: A package for evaluation of Feynman diagrams and integration over multi-particle phase space. User’s manual for version 33,” [arXiv:hep-ph/9908288]
- [11] J. Campbell and R. K. Ellis, “Next-to-leading order corrections to $W + 2\text{jet}$ and $Z + 2\text{jet}$ production at hadron colliders,” *Phys. Rev. D* **65**, 113007 (2002), [arXiv:hep-ph/0202176]
- [12] T. Junk, *Nucl. Instrum. Meth. A* **434**, 435-443 (1999)
- [13] K. S. Cranmer, *Comput. Phys. Commun.*, **136**, 198 (2001), [arXiv:hep-ph/0011057]
- [14] The procedure of replacing very low statistics MC sample shapes with a higher statistics version was performed for the following background/analysis combinations: $W/Z + 2\text{jets}$ ($WH \rightarrow e, \mu\nu b\bar{b}$); $Z \rightarrow e^+e^-, \tau^+\tau^-$ ($H \rightarrow e^+\nu e^-\nu$)
- [15] A. Read, *NIM A* 425 357-360 (1999)
- [16] DØ Collaboration, “Search for WH Production at $\sqrt{s} = 1.96 \text{ TeV}$,” DØ Conference Note 5054
- [17] DØ Collaboration, “A Search for the Standard Model Higgs boson using the $ZH \rightarrow \nu\bar{\nu}b\bar{b}$ channel in $p\bar{p}$ Collisions at $\sqrt{s} = 1.96 \text{ TeV}$,” submitted to *Phys. Rev. Lett.*, [arXiv:hep-ex/0607022]
- [18] DØ Collaboration, “A Search for $ZH \rightarrow \ell^+\ell^-b\bar{b}$ Production at DØ in $p\bar{p}$ Collisions at $\sqrt{s} = 1.96 \text{ TeV}$,” DØ Conference Note 5186
- [19] DØ Collaboration, “Search for associated Higgs boson production $WH \rightarrow WWW^* \rightarrow \ell^\pm\nu\ell^\pm\nu + X$ in $p\bar{p}$ Collisions at $\sqrt{s} = 1.96 \text{ TeV}$,” submitted to *Phys. Rev. Lett.*, [arXiv:hep-ex/0607032]
- [20] DØ Collaboration, “Search for the Higgs boson in $H \rightarrow WW^* \rightarrow l^+l^-(ee, e\mu)$ decays with 950 pb^{-1} at DØ in Run II,” DØ Conference Note 5063
- [21] DØ Collaboration, “Search for the Higgs boson in $H \rightarrow WW^* \rightarrow \mu\mu$ decays with 930 pb^{-1} at DØ in Run II,” DØ Conference Note 5194
- [22] M. Carena, J. Conway, J. Hobbs *et. al.*, FERMILAB-CONF-00/279-T (2000), [arXiv:hep-ph/0010338]
- [23] For the two $ZH \rightarrow \ell^+\ell^-b\bar{b}$ analyses, only the double-tag is considered.
- [24] The uncertainty on the expected multijet background is dominated by the statistics of the data sample from which it is estimated, and is considered separately from the other cross section uncertainties.